Pacemakers handshake synchronization mechanism of mammalian respiratory rhythmogenesis

Steffen Wittmeier[a], Gang Song[a], James Duffin[b], and Chi-Sang Poon[a,1]

[a]Harvard–MIT Division of Health Sciences and Technology, Massachusetts Institute of Technology, Cambridge, MA 02139; and [b]Departments of Physiology and Anaesthesia, University of Toronto, Toronto, ON, Canada M5S 1A8

Communicated by Masao Ito, RIKEN, Saitama, Japan, September 19, 2008 (received for review June 20, 2008)

Inspiratory and expiratory rhythms in mammals are thought to be generated by pacemaker-like neurons in 2 discrete brainstem regions: pre-Bötzinger complex (preBötC) and parafacial respiratory group (pFRG). How these putative pacemakers or pacemaker networks may interact to set the overall respiratory rhythm in synchrony remains unclear. Here, we show that a pacemakers 2-way ''handshake'' process comprising pFRG excitation of the preBötC, followed by reverse inhibition and postinhibitory rebound (PIR) excitation of the pFRG and postinspiratory feedback inhibition of the preBötC, can provide a phase-locked mechanism that sequentially resets and, hence, synchronizes the inspiratory and expiratory rhythms in neonates. The order of this handshake sequence and its progression vary depending on the relative excitabilities of the preBötC vs. the pFRG and resultant modulations of the PIR in various excited and depressed states, leading to complex inspiratory and expiratory phase-resetting behaviors in neonates and adults. This parsimonious model of pacemakers synchronization and mutual entrainment replicates key experimental data in vitro and in vivo that delineate the developmental changes in respiratory rhythm from neonates to maturity, elucidating their underlying mechanisms and suggesting hypotheses for further experimental testing. Such a pacemakers handshake process with conjugate excitation–inhibition and PIR provides a reinforcing and evolutionarily advantageous fail-safe mechanism for respiratory rhythmogenesis in mammals.

entrainment | parafacial respiratory group | postinhibitory rebound | preBötzinger complex | rhythm

Pacemaker bursting and beating are profound emergent behaviors at the single-cell level that are fundamental to a myriad of biological rhythms (1, 2). How distinct oscillators may synchronize at the network level to produce an ensemble rhythm in unison is an important question for many periodic phenomena in nature (3–5). In mammalian respiration, pacemaker-like neurons have been identified in 2 discrete regions in the rostral ventrolateral medulla (VLM): the pre-Bötzinger complex (preBötC) (6) and parafacial respiratory group (pFRG) (7–9). The demonstrated plurality of respiratory-related pacemakers has led to divergent hypotheses regarding the mechanism of respiratory rhythmogenesis in mammals: (*i*) the preBötC and pFRG rhythmogenic populations represent coupled inspiratory and expiratory rhythm generators (IRG, ERG) that separately drive inspiration and expiration (10–13); and (*ii*) pFRG neurons represent the master rhythm generator that not only sets the expiratory rhythm but also entrains inspiratory bursts (9, 14).

Both hypotheses appear to be well-founded and supported by relevant experimental data. Yet, both leave major questions unanswered. For one, how can the IRG and ERG synchronize without a master rhythm generator? Conversely, if the pFRG is a master rhythm generator, then why does breathing persist after its lesioning (9, 15)?

To resolve the dilemma, we propose a mathematical model of respiratory rhythmogenesis (Fig. 1*A*) in which the IRG and ERG work in tandem via a sequence of excitation–reverse inhibition–postinhibitory rebound (PIR) excitation, in a 2-way "handshake" process (16, 17) that sequentially resets and, hence, synchronizes the inspiratory and expiratory rhythms. We show that the proposed handshake process—in particular the PIR mechanism—provides the missing link that elucidates key experimental data in vitro and in vivo from neonates to maturity.

Results

Pacemakers Handshake Model. The preBötC and pFRG pacemaker models in Fig. 1*A* are based on Hodgkin–Huxley formalism (See *Methods* and supporting information (SI) *Text*). Bursts are controlled by persistent sodium (NaP) channels (18, 19), which are known to evoke robust PIR (20, 21)—a critical requirement of our model. Although other types of pacemaker (22, 23) or interacting nonpacemaker networks may also contribute to rhythmogenesis either singly or in a population setting (2, 24, 25), how the various putative bursting mechanisms are organized in the preBötC and the pFRG is presently unclear. Nevertheless, for the present purpose of studying the interaction of the IRG and ERG, the precise rhythmogenic mechanisms within each network are unimportant. Thus, both networks may be conveniently compartmentalized as discrete "pacemakers" of a specific type, with the stipulation that any lumped effects of the interaction should also apply at the full-blown network level (unless otherwise specified)—perhaps with an even greater degree of parameter robustness (25).

Because the preBötC pacemaker is generally less excitable than the pFRG in neonatal or juvenile animals (13, 26), it is set normally silent or at a lower spontaneous burst frequency than the pFRG. (For adult animals the reverse is true; see below.) Hence, the normal (forward) handshake sequence proceeds as follows. Initially, a pFRG preinspiratory (pre-I) excitation triggers the preBötC inspiratory burst (27, 28) which, in turn, reverse inhibits (presumably via some inhibitory interneuron) and abruptly terminates the pre-I activity and hyperpolarizes the pFRG neuron (19, 29). In contrast to previous models that incorporated similar excitatory–inhibitory interactions between the pFRG and preBötC networks (30, 31), our model postulates that the reverse inhibition subsequently reactivates the pFRG via PIR, hence resetting the post-I burst. Finally, the model assumes that a post-I feedback inhibition prevents the preBötC pacemaker from reactivation (whereas PIR in the preBötC is precluded if the inhibition is indirect especially during inactivation of the preBötC). This post-I feedback may come from primary pFRG post-I activity or putative pontine "inspiratory off-switch" activity (32), both of which may be relayed to the preBötC via inhibitory interneurons such as VLM glycinergic post-I neurons (33). The latter are believed to mediate the Hering–Breuer inflation reflex (34), which is thought to inhibit

Author contributions: S.W., J.D., and C.-S.P. designed research; S.W. and G.S. performed research; S.W., G.S., and C.-S.P. analyzed data; and C.-S.P. wrote the paper.

The authors declare no conflict of interest.

[1]To whom correspondence should be addressed. E-mail: cpoon@mit.edu.

This article contains supporting information online at www.pnas.org/cgi/content/full/0809377105/DCSupplemental.

© 2008 by The National Academy of Sciences of the USA

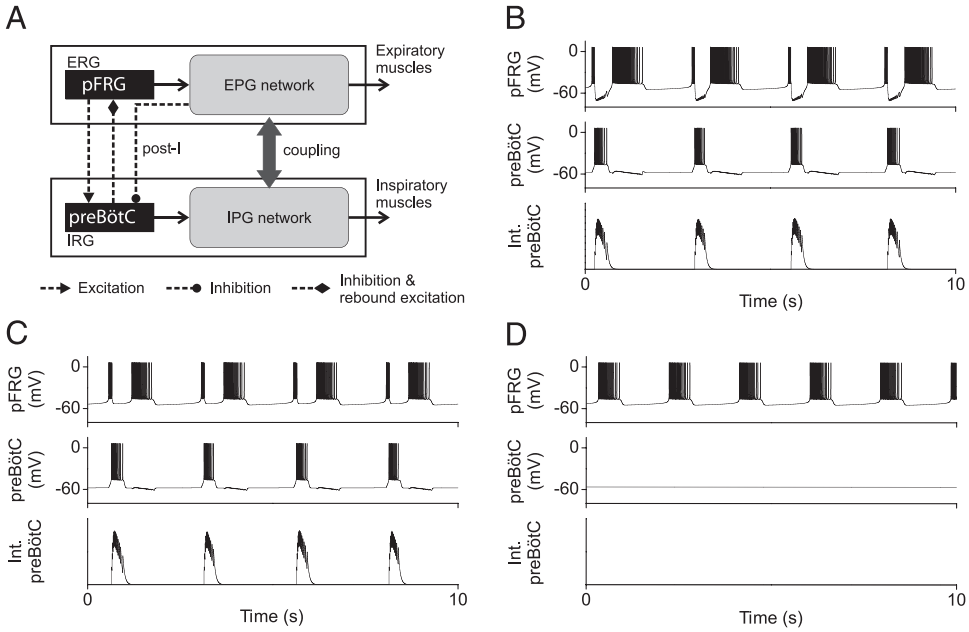

Fig. 1. Pacemakers handshake model of respiratory rhythm generation in neonates. (*A*) Pacemaker-like neurons in the pFRG and preBötC constitute the putative ERG and IRG (expiratory and inspiratory rhythm generators). EPG and IPG are expiratory and inspiratory pattern generators. PreBötC inhibits pFRG pacemaker (presumably via some inhibitory interneuron, data not shown) during the inspiratory phase and induces a PIR during the post-I phase. A post-I feedback provides a putative ''inspiratory off-switch'' through direct or indirect synaptic inhibition of the preBötC. (*B* and *C*) Model simulations of pFRG and preBötC membrane potential trajectories with alternating pre-I, inspiratory, and post-I bursts evidencing a forward handshake sequence. PIR is robustly induced with inhibitory synapse reversal potentials of −94 mV in *B* and −53mV in *C*. Int. preBötC, integrated preBötC activity. (*D*) Corresponding intrinsic pFRG membrane potential trajectories without preBötC inhibition. Duration of an uninterrupted pFRG burst (562 ms) is comparable with those of the PIR-induced post-I bursts in *B* (757 ms) and *C* (542 ms).

preBötC activity (12). Apart from this post-I feedback, details of the expiratory and inspiratory pattern generators (EPG, IPG) that shape the final respiratory pattern (Fig. 1*A*) are omitted in this minimal model of pFRG-preBötC interaction.

Pacemakers Handshake Sequence in Neonates. Model simulations mimic the experimentally observed membrane voltage trajectories of pFRG and preBötC type 1 pacemaker-like neurons in neonatal animals (Figs. 1 *B* and *C*). The sequence of biphasic (pre- and post-I) pFRG bursts interrupted by a preBötC decrementing inspiratory burst evidences a normal (forward) handshake process that alternately triggers and entrains inspiratory and expiratory activities. The duration of the post-I burst alone (not counting the pre-I and inspiratory hyperpolarization durations of the biphasic burst) is comparable with that of an intrinsic (uninterrupted) pFRG burst (Fig. 1*D*), suggesting that the post-I burst is not simply a continuation of the pre-I burst but represents PIR, which is robustly induced under a wide range of hyperpolarizing potentials from −94 mV (Fig. 1*B*) to −53 mV (Fig. 1*C*). This model prediction implies that NaP-mediated PIR could potentially underlie the post-I burst in most pFRG neurons with either weak or strong inspiratory hyperpolarization (19, 35).

On the other hand, further elevation of the inhibitory synapse reverse potential greater than −50 mV is deleterious because this may lead to depolarizing synaptic events (as seen in some immature preBötC GABAergic/glycinergic synapses; see figure 7 in ref. 36) that may impair the post-I feedback inhibition of the preBötC, causing possible reverberations of the pFRG and preBötC bursts in the post-I phase. Indeed, doublets or triplets of inspiratory activity are frequently observed in (typically younger and, hence, immature) neonatal preparations in vitro (37–39). These observations suggest that PIR of the pFRG and post-I feedback inhibition of the preBötC are indeed integral to respiratory rhythmogenesis, as postulated by our model.

Pacemakers Phase-Resetting Criticality. In a series of seminal studies Onimaru *et al.* (7, 8, 40) applied brief electrical stimuli to the pFRG region during expiration to induce resetting of pre-I and phrenic nerve firing. They found that when the stimulus was applied within ≈60% of the phrenic cycle time (T_c) the resultant expiratory duration (T_{SE}) was proportionately prolonged, whereas later stimuli evoked a premature phrenic burst. In both cases, the duration of the expiration immediately poststimulation (T_{PSE}) was unchanged. This time-critical phenomenon is accurately reproduced by our model (Fig. 2). Accordingly, pFRG stimuli applied within 66% of the preBötC cycle time ($T_s \leq 66\%$ of T_c) proportionately prolong T_{SE} (Fig. 2 *A* and *C*), whereas later stimuli evoke a premature preBötC burst that shortens T_{SE} (Fig. 2 *B* and *C*). In both cases, T_{PSE} remains unchanged (Fig. 2*C*).

Our model analyses showed that these time-dependent effects reflect the intrinsic properties of the pFRG and preBötC pacemakers, particularly their inactivation time constants [or equivalent burst-terminating dynamics at the neuronal (41) or network (42) levels]. Following a handshake, the excitability of both pacemakers gradually increases. Hence, stimuli applied later during expiration are more effective in triggering preBötC bursts as both pacemakers become more excitable (Fig. S1). These findings imply that pFRG pacing of inspiratory bursts is subject to preBötC "vetoing," i.e., the preBötC pacemaker cannot be paced prematurely if it is not yet excitable.

Opioid-Induced Fractional Quantal Slowing of Breathing. This vetoing effect is most dramatic when the preBötC is depressed. It has been demonstrated that μ-opioid agonists such as DAMGO or fentanyl evoke "quantal slowing" of breathing with random

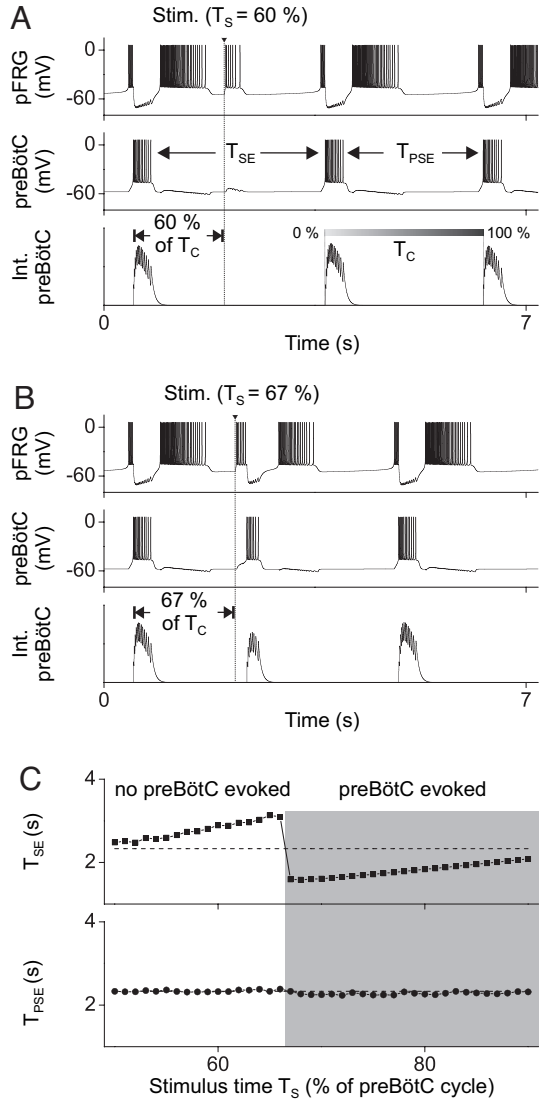

Fig. 2. Criticality of pFRG and preBötC phase resetting by brief pFRG stimulation. The model accurately simulates the experimentally observed inspiratory–expiratory phase resetting elicited by pFRG stimulation (7, 8, 40). (*A*) pFRG stimulation (amplitude, 10 pA; duration, 40 ms) within 60% of the preBötC cycle ($T_s \leq 60\%$ of T_c) resets the expiratory rhythm and prolongs the stimulated expiration. (*B*) Stimulation at T_s = 67% evokes a premature preBötC burst that terminates the expiratory phase and resets the inspiratory phase. (*C*) Summary plots showing the time-critical nature of preBötC phase resetting predicted by the model. T_{SE}, duration of the stimulated expiration. T_{PSE}, duration of the poststimulus expiration.

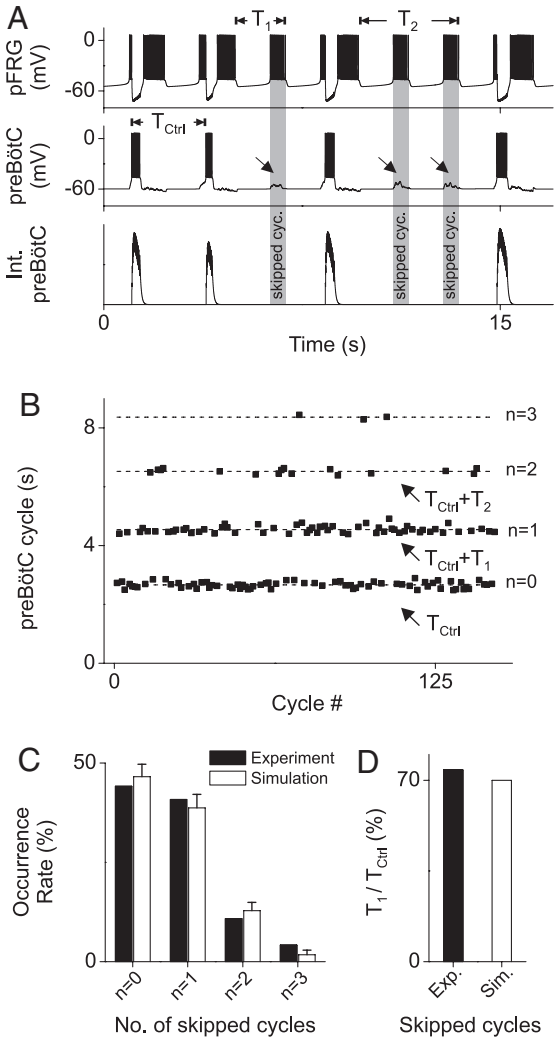

Fig. 3. Model simulation of opioid-induced fractional quantal slowing of breathing. (*A*) preBötC bursts are skipped whenever the random excitatory transmission to the depressed preBötC fails to reach the firing threshold, as indicated by the oblique arrows and shaded vertical bars. Note that the durations of the pre-I and post-I bursts for nonskipped cycles vary randomly from cycle to cycle but always in opposite directions, i.e., a shorter pre-I is followed by a longer post-I. (*B*) Quanta of preBötC cycle duration for varying skipped cycles (n = 0, 1, 2, 3). Note that the quantal increments of cycle duration (T_1, T_2, … with $T_n \approx n \cdot T_1$ and $T_1 < T_{ctrl}$) are fractional instead of integer multiples of the normal cycle duration T_{ctrl}. (*C*) Histogram of skipping 0–3 preBötC bursts in the simulation compared with similar experimental data derived from figure 2 in ref. 12. (*D*) Skipped cycle duration expressed as a percentage of normal cycle duration ($T_1/T_{ctrl} \approx 70\%$ in simulation, compared with the experimental value of ≈74% from figure 2 in ref.12).

skipped inspiratory cycles, presumably resulting from transmission failure from the periodic pFRG excitatory drive to the depressed preBötC networks (27). We have incorporated the pre- and postsynaptic depression effects of μ-opioid agonists on preBötC neurons in our model by assuming a Gaussian-distributed conductance with mean conductance increase of g_E = 0.105 nano-Siemens (nS) (87.5% of control) and variance of $g_E/2$, and a hyperpolarization of ≈3 mV. Simulation results (Fig. 3 *A* and *B*) show that quantal increases in preBötC cycle duration occur whenever the pFRG fails to excite the preBötC neuron, as observed experimentally (27, 28). Additionally, the model shows that neither pre- nor postsynaptic effects alone can totally account for the experimental distribution of respiratory cycle durations (Figs. S2 and S3); hence, both mechanisms contribute to quantal slowing of breathing (Fig. 3*C*).

A critical test of a mathematical model is its ability to not only reproduce observed data but also reinterpret or reconcile ambiguous data that cannot be explained by previous models. In this regard, our model predicts that the quantal preBötC cycle durations are not "integer multiples" of control as previously thought (27) but are fractional multiples (Fig. 3 *B* and *D*), in accord with more recent findings that contradicted previous erroneous assumptions (12). From the perspective of our model, the shorter pFRG cycle duration during a skipped preBötC cycle reflects the lack of PIR-induced resetting of the expiratory phase as part of the handshake process (Fig. 3*A*, see also Fig. 1 *B–D*). The opioid-induced fractional quantal slowing of breathing, therefore, provides strong evidence that the pFRG post-I burst

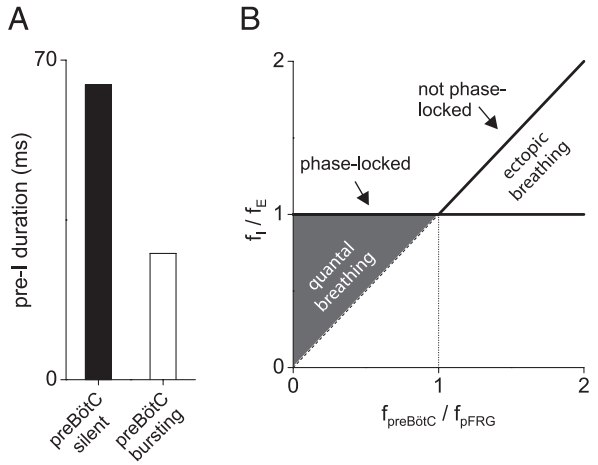

Fig. 4. pFRG initiation and preBötC veto/promotion of handshake. (*A*) Durations of the pre-I burst when the preBötC is silent ($E_{Leak\text{-}preBötC} = -61$mV as in Figs. 1–3) and when it is spontaneously bursting ($E_{Leak\text{-}preBötC} = -59$mV). (*B*) Model prediction of pFRG-preBötC phase locking with full handshake sequence present and the lack of phase locking during quantal breathing (preBötC-depressed) or ectopic breathing (preBötC-stimulated). The thick lines indicate the predicted relations when the preBötC is not depressed. Normally, the preBötC's spontaneous burst frequency is lower than the pFRG's ($f_{preBötC} < f_{pFRG}$); hence the inspiratory rhythm is always entrained by the expiratory rhythm to the same frequency ($f_I/f_E = 1$). During quantal breathing the pre-I input is occasionally vetoed by the preBötC for lack of excitability and hence $f_I/f_E < 1$. When the preBötC network is excited such that $f_{preBötC} > f_{pFRG}$ (while the pFRG remains fairly excitable to entrain the preBötC), the inspiratory rhythm has two components: a weak, free-running ectopic rhythm (identity line) produced by the asynchronous preBötC network and a ''normal'' rhythm that remains phased-locked to the expiratory rhythm (horizontal line). These model predictions are in agreement with experimental observations reported in ref. 12.

is not merely a continuation of the pre-I burst (or driven by other uninhibited pFRG neurons) but is actively refreshed (hence prolonged) by PIR (Fig. 1 *B–D*). The close agreement between the predicted and observed fractional quantal cycle durations (Fig. 3*D*) lends further support for an important role of PIR-induced expiratory phase resetting in respiratory rhythmogenesis.

Initiation, Vetoing, and Promotion of Handshake. Much as the preBötC may veto a handshake, a higher preBötC excitability may also promote its development. Fig. 4*A* shows that pre-I activity is cut short when preBötC excitability is increased (to spontaneous bursting), in agreement with the reported age-dependent reduction and μ-opioid-dependent augmentation of pre-I activity (43). Correspondingly, pFRG post-I activity is augmented, as the resultant increased preBötC inhibition of the pFRG leads to increased PIR. These predicted effects are evident in Fig. 3*A*, where the durations of the pFRG pre- and post-I bursts (for nonskipped cycles) are seen to vary reciprocally from cycle to cycle, reflecting the random fluctuations of preBötC excitation.

This handshake sequence, when fully operative, always keeps the resultant preBötC rhythm phase-locked to the pFRG rhythm either 1:1 or quantally when depressed (Fig. 4*B*). However, a question arises as to whether the preBötC could pace the pFRG when it becomes more excitable. Janczewski and Feldman (12) used lung deflation or the μ-opioid antagonist naloxone to raise the inspiratory frequency (f_I) above the expiratory frequency (f_E) in vagi-intact juvenile rats given fentanyl. In both cases, the inspiratory rhythm outpaced the expiratory rhythm with weak and erratic ectopic inspirations in between (not phase-locked), whereas all expiratory bursts continued to entrain strong inspiratory bursts (phase-locked) as in the forward handshake sequence.

These experimental observations are at variance with previous hypotheses (9–14) but have 2 important implications from the perspective of the present model. First, although the preBötC is capable of bursting faster than the pFRG asynchronously under certain conditions, strong inspiratory bursts are contingent on expiratory triggering. A possible explanation is that inspiratory bursts are strongest when the preBötC rhythmogenic network is synchronized (36) by a pre-I trigger. Second, free-running ectopic inspiratory bursts do not readily entrain the expiratory rhythm or activate an interaction with the pFRG. A possible explanation is that PIR of the pFRG may fail to develop if inspiratory inhibition (from ectopic bursts) is relatively weak, especially when the pFRG is inactivated. Taken together, these observations support the model prediction (Fig. 4 *A* and *B*) that the forward handshake process, although it is subject to preBötC excitability, is normally always triggered by pre-I activity provided the pFRG is relatively excitable (as in neonatal or juvenile animals), regardless of whether the pFRG bursts faster than the preBötC network ($f_{pFRG} > f_{preBötC}$) or not.

Latent Handshake Processes in Maturity. In adult animals, however, the pFRG is normally depressed, and the more excitable preBötC becomes dominant (10, 12). Under those circumstances, the forward handshake might degenerate to less-tightly coupled handshake processes with anomalous preBötC–pFRG phase-resetting patterns. First, when the pFRG is sufficiently depressed the preBötC could set the respiratory rhythm without evoking PIR and hence, no handshake can be observed (Fig. 5*A*). Indeed, such quiescent ''pre-I'' neurons are intrinsically indiscernible, hence the reported lack of pre-I activity under normal conditions in adult animals (44).

When the pFRG is gradually relieved (by hypoxia or other stimulants) from depression, however, our model predicts a series of increasingly intertwined preBötC–pFRG interactions. Specifically, when the depressed pFRG excitability is partially restored to a narrow band between 2 closely spaced transition thresholds, a peculiar ''reverse handshake'' sequence with contiguous inspiratory–expiratory–inspiratory activities ensues (Fig. 5*B*). Under those rare conditions, spontaneous preBötC activity may induce PIR in the pFRG, which, in turn, could evoke a second preBötC burst in the absence of an inspiratory off-switch. The increased inactivation of the preBötC after the double bursts delays the onset of subsequent preBötC activation, resulting in increased interburst interval and hence decreased respiratory frequency. Evidence for such a unique double-burst inspiratory pattern with bradypnea is provided by preliminary data in adult rats after severe hypoxia in vivo (Fig. S4). Similar doublets of inspiratory activity with depressed pre-I and augmented post-I expiratory (lumbar) activities and decreased respiratory frequency have also been reported in newborn rat brainstem–spinal cord preparations in vitro (45). This remarkable bimodal inspiratory rhythm as predicted by our model cannot be explained by previous models of respiratory rhythm generation, and suggests a critical test for future studies to identify the developmental changes of the pFRG pacemaker from neonates to maturity.

Furthermore, when pFRG excitability is restored even further from depression, the model predicts that the reverse handshake sequence may convert to a ''half handshake'' (Fig. 5*C*). In this circumstance, the pFRG may again trigger the handshake sequence as with the forward handshake sequence (when the pFRG is highly excitable). However, the leading pFRG burst in this case is not a spontaneous pre-I burst but a delayed PIR from the preceding preBötC inhibition (which hastens pFRG neuron inactivation). In this manner the pFRG may burst faster than the preBötC (hence accelerating the respiratory frequency) even

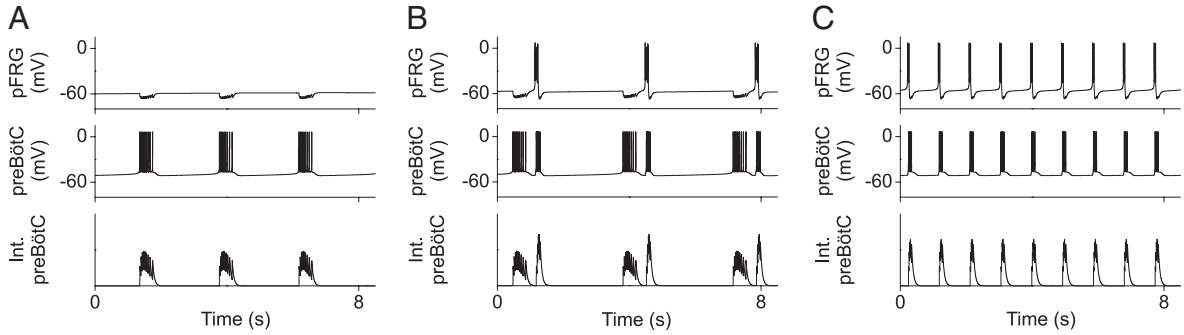

Fig. 5. Simulation of no, reverse, and half handshakes when the preBötC is more excitable than the pFRG. Simulation settings are: $E_{\text{Leak-preBötC}} = -57.0$ mV, $g_{\text{I}} = 0.5$ nS. (*A*) No handshake. When the pFRG is sufficiently depressed ($E_{\text{Leak-pFRG}} \leq -64.0$ mV) the preBötC becomes the only active pacemaker that drives the respiratory rhythm. (*B*) Reverse handshake. When the pFRG excitability is partially restored ($E_{\text{Leak-pFRG}} = -63.2$ mV) the driving preBötC burst may induce PIR of the pFRG which, in turn, triggers a second preBötC burst in the absence of post-I inhibition of the preBötC. This peculiar phenomenon occurs only within a narrow band of depressed pFRG excitability relative to preBötC and hence, is rarely discernible experimentally (although a wider band may be possible in full-blown pFRG and preBötC population networks). (*C*) Half handshake. At even less depressed pFRG excitability levels ($E_{\text{Leak-pFRG}} = -62.3$ mV) the pFRG-triggered preBötC burst may induce a delayed PIR of the pFRG which, in turn, triggers a new preBötC burst, and so on.

though it is intrinsically less excitable than the preBötC. Thus, pacemakers interaction per se may lead to either bradypnea or tachypnea (Fig. 5 *B* and *C*) during respiratory stimulation. These distinctive model predictions suggest yet another critical experimental test of the model in future.

Finally, when the pFRG pacemaker is preferentially stimulated such that it becomes more excitable than the adult preBötC pacemaker (with $f_{\text{pFRG}} > f_{\text{preBötC}}$), the model predicts that the forward handshake process normally found in neonates may reappear. It has been recently reported that some expiratory-augmenting neurons in the Bötzinger complex of adult rats may exhibit (after exposure to severe hypercapnic hypoxia) biphasic pre- and post-I-like activities that are reminiscent of neonatal pFRG activities (44). However, as pointed out in ref. 46, because those expiratory-augmenting neurons are glycinergic, they are unlikely the mature form of neonatal pFRG pacemaker neurons that are presumably excitatory [although neurons could coexpress both excitatory and inhibitory neurotransmission (47)]. Nevertheless, some expiratory-augmenting excitatory (bulbospinal) neurons in the caudal VLM do reportedly demonstrate pre-I activity (with a half handshake-like sequence similar to Fig. 5*C*) or biphasic pre- and post-I activities (similar to a forward handshake) during or after severe hypercapnic hypoxia (44). Whether such adult forms of pre- and/or post-I expiratory premotor activities are related to neonatal pFRG activities remains to be clarified, although pre-I premotor neurons are also found in the caudal VLM of neonates (29).

Discussion

Minimal Model of Respiratory Rhythmogenesis in Neonatal and Adult Animals. A cardinal principle (Occam's razor) underlying the use of mathematical modeling to convey mechanistic insight is to keep the model as simple as possible (i.e., "minimal model") but as complex as needed to describe the critical features of the system and resultant data (48). The present model was constructed with only sufficient complexity to demonstrate the ability of the hypothesized interactions to reproduce experimental results and predict new results. Therefore, details of the IPG and EPG are not explicitly represented here, except a post-I feedback signal is postulated to provide a backup "inspiratory off-switch" that prevents the IRG from reactivation. The use of NaP for the bursting and PIR mechanisms is an assumption, as is the pacemaker concept itself, and these could be replaced by other pacemaker mechanisms or group pacemaker/nonpacemaker mechanisms for parameter robustness (25) and network synchrony (36). Nevertheless, the hypothesized excitatory–inhibitory interaction along with PIR excitation and post-I feedback inhibition would still apply, and it is those that we wished to test, so the current parsimonious model sufficed. The remarkable versatility of this minimal model is evidenced by its ability to faithfully reproduce a wide range of experimentally observed behaviors with both in vitro and in vivo preparations ranging in age from neonatal to adult. These behaviors (particularly the opioid-induced fractional quantal slowing effect in neonates and the hypoxia-induced reverse handshake effect in adults) cannot be explained by previous models of respiratory rhythmogenesis based on isolated or coupled pacemakers (9, 10, 12, 30, 31) or other pacemaker and nonpacemaker networks without PIR (25, 49–51).

Implications of Pacemakers Handshake Model. The present results demonstrate a handshake mechanism of respiratory pacemakers synchronization and mutual entrainment in neonatal and adult animals. Specifically, our model suggests that the IRG and ERG are neither autonomous nor master–slave to one another as previously thought but, instead, may interact via conjugate excitation–inhibition and, most importantly, an ensuing PIR excitation to provide a harmonious respiratory rhythm with phase-locked inspiratory and expiratory activities. This notion is supported by the recent finding that mutant fetal mice with defective pFRG–preBötC interaction do not produce rhythmic phrenic activity (52). Such a pacemakers 2-way handshake process based on conjugate excitation–inhibition [instead of reciprocal inhibition (53, 54)] with PIR is beneficial for animal survival in that the excitatory pre-I activity may help to synchronize the preBötC rhythmogenic network. Although the preBötC is thought to be critical for inspiratory activity (55), inspiratory bursts that are triggered by pre-I activity prove stronger, more regular, and more robust than otherwise particularly when the preBötC is depressed (12), as in neonates (10, 13). In adult animals, the handshake process is latent but may be reactivated to assume varying forms when the respiratory system is challenged (either chemically or mechanically) such that inspiratory drive alone becomes nonoptimal or ineffective, and recruitment of expiratory activity is necessary to sustain breathing (56). Such a pacemakers handshake process, therefore, provides an advantageous fail-safe mechanism that may sustain or augment breathing should the preBötC be insufficient or fail. We suggest that such fail-safe redundancy in pacemakers network design may be evolutionarily conserved with possible heritage from early ancestors, such as frogs and fish (57).

Methods

Model Parameters. Each ''pacemaker'' in Fig. 1*A* consists of a membrane capacitance with fast sodium NaF, delayed rectifier potassium KDr, persistent sodium NaP, and leak channels as described previously (20) (corresponding equations and parameter values are found in *SI Text* and Table S1). In addition, the reversal potential of the excitatory synapse was set to −10 mV, whereas that of the inhibitory synapses was −94 mV (as in ref. 58) or −53 mV (assuming GABAergic or glycinergic inhibition). Because the specific receptor subtypes of pFRG-preBötC synaptic interactions have not been identified, the time-dependent changes in synaptic conductance was modeled by a single exponential with decay time constant of 25 ms to broadly cover both fast and slow excitatory and inhibitory receptor currents as in ref. 58. The synaptic conductance increase associated with one synaptic event was set to $g_E = 0.12$ nS for the excitatory synapse and $g_I = 1$ nS for the inhibitory synapses, unless specified otherwise.

Model Simulation. Simulations were performed on the NEURON simulator platform (59) using the 2nd-order accurate Crank–Nicholson integration scheme with a time-step of 25 μs.

ACKNOWLEDGMENTS. We thank J. Champagnat for helpful comments on the manuscript. This work was supported by National Institutes of Health Grants HL067966, HL072849, HL079503, and EB005460.

1. Czeisler CA, *et al.* (1999) Stability, precision, and near-24-hour period of the human circadian pacemaker. *Science* 284:2177–2181.
2. Ramirez JM, Tryba AK, Pena F (2004) Pacemaker neurons and neuronal networks: An integrative view. *Curr Opin Neurobiol* 14:665–674.
3. Strogatz SH, Stewart I (1993) Coupled oscillators and biological synchronization. *Sci Am* 269(6):102–109.
4. Matsugu M, Duffin J, Poon CS (1998) Entrainment, instability, quasi-periodicity, and chaos in a compound neural oscillator. *J Comput Neurosci* 5:35–51.
5. MacDonald SM, Song G, Poon CS (2007) Nonassociative learning promotes respiratory entrainment to mechanical ventilation. *PLoS ONE* 2:e865.
6. Smith JC, Ellenberger HH, Ballanyi K, Richter DW, Feldman JL (1991) Pre-Botzinger complex: a brainstem region that may generate respiratory rhythm in mammals. *Science* 254:726–729.
7. Onimaru H, Arata A, Homma I (1987) Localization of respiratory rhythm-generating neurons in the medulla of brainstem-spinal cord preparations from newborn rats. *Neurosci Lett* 78:151–155.
8. Onimaru H, Arata A, Homma I (1988) Primary respiratory rhythm generator in the medulla of brainstem-spinal cord preparation from newborn rat. *Brain Res* 445:314–324.
9. Onimaru H, Homma I (2003) A novel functional neuron group for respiratory rhythm generation in the ventral medulla. *J Neurosci* 23:1478–1486.
10. Feldman JL, Del Negro CA (2006) Looking for inspiration: New perspectives on respiratory rhythm. *Nat Rev* 7:232–242.
11. Janczewski WA, Feldman JL (2006) Novel data supporting the two respiratory rhythm oscillator hypothesis. Focus on ''respiration-related rhythmic activity in the rostral medulla of newborn rats''. *J Neurophysiol* 96:1–2.
12. Janczewski WA, Feldman JL (2006) Distinct rhythm generators for inspiration and expiration in the juvenile rat. *J Physiol* 570(Pt 2):407–420.
13. Feldman JL, Janczewski WA (2006) Point:Counterpoint: The parafacial respiratory group (pFRG)/pre-Botzinger complex (preBotC) is the primary site of respiratory rhythm generation in the mammal. Counterpoint: the preBotC is the primary site of respiratory rhythm generation in the mammal. *J Appl Physiol* 100:2096–2097; discussion 2097–2098:2103–2108.
14. Onimaru H, Homma I (2006) Point:Counterpoint: The parafacial respiratory group (pFRG)/pre-Botzinger complex (preBotC) is the primary site of respiratory rhythm generation in the mammal. Point: the PFRG is the primary site of respiratory rhythm generation in the mammal. *J Appl Physiol* 100:2094–2095.
15. Chatonnet F, *et al.* (2003) From hindbrain segmentation to breathing after birth: Developmental patterning in rhombomeres 3 and 4. *Mol Neurobiol* 28:277–294.
16. Berkel Kv (1993) *Handshake Circuits : An Asynchronous Architecture for VLSI Programming* (Cambridge Univ Press, Cambridge, UK) pp xiv, 225.
17. Sparsø J, Furber SB (2001) *Principles of Asynchronous Circuit Design : A Systems Perspective* (Kluwer Academic, Boston) pp xx, 337.
18. Rybak IA, Ptak K, Shevtsova NA, McCrimmon DR (2003) Sodium currents in neurons from the rostroventrolateral medulla of the rat. *J Neurophysiol* 90:1635–1642.
19. Onimaru H, Arata A, Homma I (1997) Neuronal mechanisms of respiratory rhythm generation: An approach using in vitro preparation. *Jpn J Physiol* 47:385–403.
20. Butera RJ, Jr, Rinzel J, Smith JC (1999) Models of respiratory rhythm generation in the pre-Botzinger complex. I. Bursting pacemaker neurons. *J Neurophysiol* 82:382–397.
21. Wu N, *et al.* (2005) Persistent sodium currents in mesencephalic v neurons participate in burst generation and control of membrane excitability. *J Neurophysiol* 93:2710–2722.
22. Thoby-Brisson M, Ramirez JM (2001) Identification of two types of inspiratory pacemaker neurons in the isolated respiratory neural network of mice. *J Neurophysiol* 86:104–112.
23. Del Negro CA, *et al.* (2005) Sodium and calcium current-mediated pacemaker neurons and respiratory rhythm generation. *J Neurosci* 25:446–453.
24. Del Negro CA, Morgado-Valle C, Feldman JL (2002) Respiratory rhythm: An emergent network property? *Neuron* 34:821–830.
25. Purvis LK, Smith JC, Koizumi H, Butera RJ (2007) Intrinsic bursters increase the robustness of rhythm generation in an excitatory network. *J Neurophysiol* 97:1515–1526.
26. Onimaru H, Arata A, Homma I (1989) Firing properties of respiratory rhythm generating neurons in the absence of synaptic transmission in rat medulla in vitro. *Exp Brain Res* 76:530–536.
27. Mellen NM, Janczewski WA, Bocchiaro CM, Feldman JL (2003) Opioid-induced quantal slowing reveals dual networks for respiratory rhythm generation. *Neuron* 37:821–826.
28. Takeda S, *et al.* (2001) Opioid action on respiratory neuron activity of the isolated respiratory network in newborn rats. *Anesthesiology* 95:740–749.
29. Janczewski WA, Onimaru H, Homma I, Feldman JL (2002) Opioid-resistant respiratory pathway from the preinspiratory neurones to abdominal muscles: in vivo and in vitro study in the newborn rat. *J Physiol* 545(Pt 3):1017–1026.
30. Bose A, Lewis T, Wilson R (2005) Two-oscillator model of ventilatory rhythmogenesis in the frog. *Neurocomputing* 65:751–757.
31. Joseph IM, Butera RJ (2005) A simple model of dynamic interactions between respiratory centers. *Conf Proc IEEE Eng Med Biol Soc* 6:5840–5842.
32. Dutschmann M, Herbert H (2006) The Kolliker-Fuse nucleus gates the postinspiratory phase of the respiratory cycle to control inspiratory off-switch and upper airway resistance in rat. *Eur J Neurosci* 24:1071–1084.
33. Ezure K, Tanaka I, Kondo M (2003) Glycine is used as a transmitter by decrementing expiratory neurons of the ventrolateral medulla in the rat. *J Neurosci* 23:8941–8948.
34. Hayashi F, Coles SK, McCrimmon DR (1996) Respiratory neurons mediating the Breuer-Hering reflex prolongation of expiration in rat. *J Neurosci* 16:6526–6536.
35. Onimaru H, Ballanyi K, Richter DW (1996) Calcium-dependent responses in neurons of the isolated respiratory network of newborn rats. *J Physiol* 491(Pt 3):677–695.
36. Wallen-Mackenzie A, *et al.* (2006) Vesicular glutamate transporter 2 is required for central respiratory rhythm generation but not for locomotor central pattern generation. *J Neurosci* 26:12294–12307.
37. Onimaru H, Kumagawa Y, Homma I (2006) Respiration-related rhythmic activity in the rostral medulla of newborn rats. *J Neurophysiol* 96:55–61.
38. Yamamoto Y, Onimaru H, Homma I (1992) Effect of substance P on respiratory rhythm and pre-inspiratory neurons in the ventrolateral structure of rostral medulla oblongata: An in vitro study. *Brain Res* 599:272–276.
39. Hamada O, Garcia-Rill E, Skinner RD (1992) Respiration in vitro: I. Spontaneous activity. *Somatosens Mot Res* 9:313–326.
40. Onimaru H, Homma I (1987) Respiratory rhythm generator neurons in medulla of brainstem-spinal cord preparation from newborn rat. *Brain Res* 403:380–384.
41. Rachmuth G, Poon C (2008) Transistor analogs of emergent iono-neuronal dynamics. *HFSP J* 2:156–166.
42. Koizumi H, Smith JC (2008) Persistent Na^+ and K^+-dominated leak currents contribute to respiratory rhythm generation in the pre-Botzinger complex in vitro. *J Neurosci* 28:1773–1785.
43. Oku Y, Masumiya H, Okada Y (2007) Postnatal developmental changes in activation profiles of the respiratory neuronal network in the rat ventral medulla. (Translated from Eng) *J Physiol* 585:175–186.
44. Fortuna MG, West GH, Stornetta RL, Guyenet PG (2008) Botzinger expiratory-augmenting neurons and the parafacial respiratory group. *J Neurosci* 28:2506–2515.
45. Taccola G, Secchia L, Ballanyi K (2007) Anoxic persistence of lumbar respiratory bursts and block of lumbar locomotion in newborn rat brainstem spinal cords. *J Physiol* 585(Pt 2):507–524.
46. Ezure K (2004) Reflections on respiratory rhythm generation. *Prog Brain Res* 143:67–74.
47. Sandler R, Smith AD (1991) Coexistence of GABA and glutamate in mossy fiber terminals of the primate hippocampus: An ultrastructural study. *J Comp Neurol* 303:177–192.
48. Pugh EN, Jr, Andersen OS (2008) Models and mechanistic insight. *J Gen Physiol* 131:515–519.
49. Richter DW, Spyer KM (2001) Studying rhythmogenesis of breathing: comparison of in vivo and in vitro models. *Trends Neurosci* 24:464–472.
50. Duffin J (2004) Functional organization of respiratory neurones: A brief review of current questions and speculations. *Exp Physiol* 89:517–529.
51. Smith JC, Abdala AP, Koizumi H, Rybak IA, Paton JF (2007) Spatial and functional architecture of the mammalian brain stem respiratory network: A hierarchy of three oscillatory mechanisms. *J Neurophysiol* 98:3370–3387.
52. Onimaru H, Ikeda K, Kawakami K (2007) Defective interaction between dual oscillators for respiratory rhythm generation in Na^+,K^+-ATPase {alpha}2 subunit-deficient mice. *J Physiol* 584(Pt 1):271–284.
53. Perkel DH, Mulloney B (1974) Motor pattern production in reciprocally inhibitory neurons exhibiting postinhibitory rebound. *Science* 185:181–183.
54. Satterlie RA (1985) Reciprocal inhibition and postinhibitory rebound produce reverberation in a locomotor pattern generator. (Translated from Eng) *Science* 229:402–404.
55. Gray PA, Janczewski WA, Mellen N, McCrimmon DR, Feldman JL (2001) Normal breathing requires preBotzinger complex neurokinin-1 receptor-expressing neurons. *Nat Neurosci* 4:927–930.
56. Poon CS, Tin C, Yu Y (2007) Homeostasis of exercise hyperpnea and optimal sensorimotor integration: The internal model paradigm. *Respir Physiol Neurobiol* 159:1–13; discussion 14–20.
57. Wilson RJ, Vasilakos K, Remmers JE (2006) Phylogeny of vertebrate respiratory rhythm generators: The oscillator homology hypothesis. *Resp Physiol Neurobiol* 154:47–60.
58. Rybak IA, Paton JF, Schwaber JS (1997) Modeling neural mechanisms for genesis of respiratory rhythm and pattern. I. Models of respiratory neurons. *J Neurophysiol* 77:1994–2006.
59. Carnevale T, Hines M (2006) *The NEURON Book* (Cambridge Univ Press, Cambridge, UK).